Journal of Zhejiang University-SCIENCE A (Applied Physics & Engineering)
ISSN 1673-565X (Print); ISSN 1862-1775 (Online)
www.zju.edu.cn/jzus; www.springerlink.com
E-mail: jzus@zju.edu.cn

Naphthalene decomposition in a DC corona radical shower discharge*

Ming-jiang NI[1], Xu SHEN[1], Xiang GAO[†‡1], Zu-liang WU[1,2], Hao LU[1,2], Zhong-shan LI[3], Zhong-yang LUO[1], Ke-fa CEN[1]

([1]*State Key Laboratory of Clean Energy Utilization, Zhejiang University, Hangzhou 310027, China*)

([2]*College of Environmental Science and Engineering, Zhejiang Gongshang University, Hangzhou 310015, China*)

([3]*Division of Combustion Physics, Lund University, S-22100 Lund, Sweden*)

[†]E-mail: xgao1@zju.edu.cn

Received Mar. 10, 2010; Revision accepted July 15, 2010; Crosschecked Dec. 7, 2010

Abstract: The naphthalene decomposition in a corona radical shower discharge (CRS) was investigated, with attention paid to the influences of voltage and initial naphthalene density. The OH emission spectra were investigated so as to know the naphthalene decomposing process. The by-products were analyzed and a decomposing theory in discharge was proposed. The results showed that higher voltage and relative humidity were effective on decomposition. The initial concentration affected the decomposing efficiency of naphthalene. When the initial naphthalene density was 17 mg/m^3, the decomposition rate was found to be 70% under 14 kV. The main by-products were carbon dioxide and water. However, a small amount of carbonic oxide, 1,2-ethanediol and acetaldehyde were found due to the incomplete oxidization.

Key words: Naphthalene decomposition, Corona, Discharge, OH radical
doi:10.1631/jzus.A1010009 **Document code:** A **CLC number:** X192

1 Introduction

Recently, controls of polycyclic aromatic hydrocarbons (PAHs) have attracted increased attention due to the progressively stringent environmental standard restriction (Aranda *et al.*, 2009; Hwang *et al.*, 2009; Nishino *et al.*, 2009). There are many technologies for PAHs removal, such as active carbon adsorption (Gong *et al.*, 2007), electron beam method (Nichipor *et al.*, 2002), and catalytic combustion (Mastral *et al.*, 2001; García *et al.*, 2006). One technique is called the corona radical shower (CRS) discharge, in which nozzle-type electrodes are used for additional gaseous injection. O_2, H_2O, N_2, NH_3, and CH_4 have been experimentally investigated as the additional gases to generate selectively initial radicals, which can react with pollutants. Studies on removal of pollutants such as NO_x, SO_2, and volatile organic compounds (VOCs) have been demonstrated (Urashima and Chang, 2000; Chang *et al.*, 2003; Wu *et al.*, 2005; Mista and Kacprzyk, 2008).

In this study, naphthalene was used for investigation, and its decomposing process was discussed in a direct current (DC) CRS discharge. To investigate the reaction between the radicals generated in discharge and naphthalene molecules, OH as the radical was detected by an optical emission spectroscopy (OES) method. The decomposing by-products were detected by a Fourier transform infrared spectroscopy (FTIR) and gas chromatography with mass spectrometric detection (GC-MS).

2 Experimental setup

The schematic diagram of the experimental apparatus is illustrated in Fig. 1. This system was

‡ Corresponding author

* Project supported by the National Basic Research Program (973) of China (No. 2006CB200303), the Chinese-Slovak Scientific and Technological Cooperation Program (No. 2010DFA92020), and the China Postdoctoral Science Foundation (No. 20100471698)

composed of a gas system, a CRS reactor, a gas analyzing system for the treated gases, and an OES.

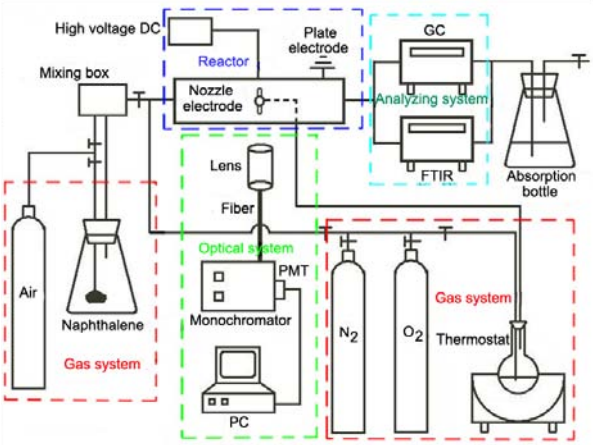

Fig. 1 Experimental system of naphthalene decomposition

The gas system included two independent parts for background gas and additional gas. Naphthalene/Air was introduced into the reactor as the background gas. The naphthalene explosive limit was between 0.88% and 5.9% (v/v), and the vapor pressure of naphthalene at ambient condition was 11 Pa. Hence, for naphthalene controlling, the naphthalene was wrapped in a water bath. Different additional gases were sprayed into the reactor through nozzles and water was bubbled into the reactor by thermostat. In this experiment, the temperature was 25 °C, and the pressure was 1.013×10^5 Pa. The decomposing by-products were captured by a gas bag and dichloromethane solution, and analyzed by the FTIR (Necolet nexus spectrometer, Germany) and GC-MS (Thermo Fisher Scientific, USA). The quantitative analysis of CO_2 was detected by GASMET-DX4000 (Gasmet Technologies Oy, Finland). Chromatographic separation was carried out on a 30 m TR-5MS capillary column with an internal diameter of 0.25 mm and a stationary phase film thickness of 0.25 μm. The temperature program for GC oven was an initial temperature 70 °C, held for 5 min; 70–270 °C at 8 °C /min; 270 °C, held for 30 min. Carrier gas: helium, 1 ml/min. The injector temperature was set to 250 °C. Mass spectrometer working condition: electron impact ionization, 70 eV; ion source temperature, 200 °C. The molecular weight range was selected from 40 to 300. The decomposing rate of naphthalene was defined as

$$\eta = \frac{c_{\text{in}} - c_{\text{out}}}{c_{\text{in}}}, \quad (1)$$

where c_{in} and c_{out} are naphthalene concentrations of the inlet and outlet, respectively.

The CRS chamber was made of plexiglass, and the space inside the CRS reactor was 200 mm×50 mm ×50 mm. Two stainless steel plates were in the two inner sides of the reactor as cathode. A stainless steel pipe with four equispaced nozzles (length, 5 mm; outer diameter, 2 mm; inner diameter, 1.8 mm) was used as anode. A quartz window was affixed on one side of the CRS chamber for optical access. The nozzle-to-plate spacing was 20 mm.

The optical diagnostic system consisted of a quartz window, two quartz lenses with diameters and focus lengths of Φ=25.4 mm, f=38.1 mm and Φ=25.4 mm, f=75 mm, respectively, a 3-axis fine adjustable platform with up to 0.625 μm resolution and a Zolix SBP 300-Spectrometer (Zolix, China) (1200 l/mm grating groove, 300 nm blazing wavelength and a CR131 photomultiplier (PMT) tube).

3 Results and discussion

3.1 Decomposition of naphthalene

3.1.1 Influence of initial concentration on naphthalene decomposition

In this condition, the background gas was naphthalene/air with a flow rate of 5 L/min, while the additional gas was humid O_2 (relative humidity (RH) =80%) with a flow of 0.5 L/min. As shown in Fig. 2, the decomposing rate of naphthalene decreased from 69% to 35% when the initial density increased from 17 to 50 mg/m^3 (Gao *et al.*, 2009). The results could be explained as follows: There were many radicals in the discharge process. Assuming the generating rate of active radicals was the same when other conditions remained unchanged, the naphthalene decomposition needed more radicals when the initial density increased. Hence, the decomposing rate decreased. In our experiment, the energy density was 5.5 Wh/m^3, so that the naphthalene destruction energy efficiency was 3.2 g/kWh when the initial concentration was 50 mg/m^3. The naphthalene removal was studied by a DC gliding arc gas discharge where the energy efficiency was 2.8 g/kWh (Yu *et al.*, 2010). Therefore,

the DC CRS discharge is effective for naphthalene decomposition.

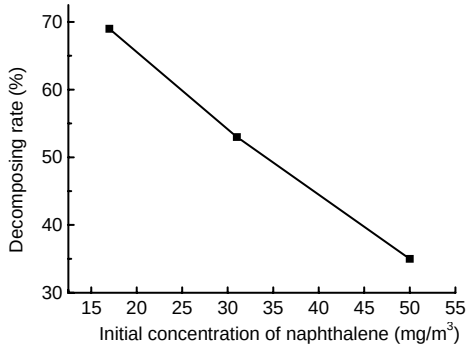

Fig. 2 Influence of the initial concentration on naphthalene decomposition (applied voltage=14 kV)

3.1.2 Influence of applied voltage on naphthalene decomposition

In this experiment, the gas condition was the same as that in Section 3.1.1. Fig. 3 shows the influence of applied voltage on naphthalene decomposition (initial concentration=17 mg/m^3) (Gao *et al.*, 2009). The decomposing rate improved from 32% to 69%, as the applied voltage increased from 8 to 14 kV. The reason was that the increased voltage could enhance the corona discharge. Thus, there would be more active radicals generated under higher voltage. The influence of discharge voltage on radical generation will be discussed later.

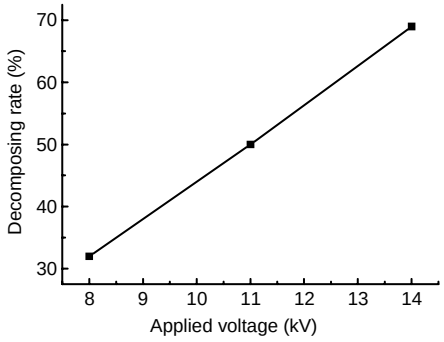

Fig. 3 Influence of the applied voltage on naphthalene decomposition (initial concentration=17 mg/m^3)

In the process of naphthalene decomposition, there are many radials involved. OH radicals play an important role. To investigate the radical generation under different voltages, emission intensity of OH radicals was observed by the OES method. In this experiment, the background gas was N_2 (5 L/min) and the additional gas was humid N_2 (0.5 L/min, RH= 80%). The spectra were collected at 25 °C and 1.013×10^5 Pa. Fig. 4 illustrates the OH ($A^2\Sigma^+\rightarrow X^2\Pi$) emission spectra under different applied voltages (Gao *et al.*, 2009). The four wavelength band heads were 306.537 nm, 306.776 nm, 307.844 nm, 308.986 nm (Pellerin *et al.*, 1996; Izarra, 2000), respectively. As shown in Fig. 4, the peaks of 309 nm (Ershov and Borysow, 1995; Falkenstein, 1997) were obvious. The dashed lines represented simulated OH emission spectra with LIFBASE fitted to the respective spectra. The peaks from 314 to 318 nm were the second positive band of N_2 ($C^3\Pi_u\rightarrow B^3\Pi_g$). The emission intensity of OH around 309 nm increased with the increased applied voltage. The relationship between the emission intensity and the concentration of excited OH radicals was as follows:

$$I_{\text{A-X}} \propto \frac{A_{\text{A-X}}}{(A_{\text{A-X}}+Q_{\text{A-X}})} h\nu_{\text{A-X}} N_{\text{A}}, \qquad (2)$$

where $I_{\text{A-X}}$, $A_{\text{A-X}}$, $Q_{\text{A-X}}$, $\nu_{\text{A-X}}$, N_{A} and h were the observed emission intensity, the Einstein coefficients, the quenching rate coefficient, the transition frequency from A to X, the concentration of excited radicals, and the Plank constant, respectively. Therefore, the emission intensity of OH (A) was proportional to the concentration of excited OH of A state.

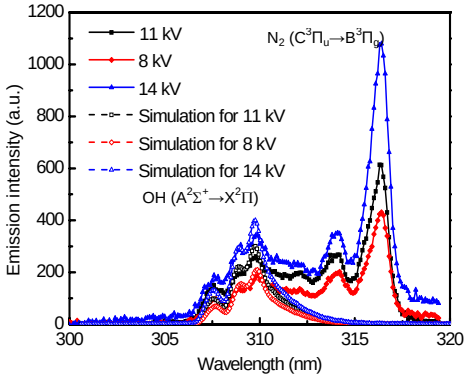

Fig. 4 Emission spectra of OH radicals under different applied voltages

The variation of OH intensity with applied voltage compared with the decomposing rate is shown in Fig. 5 (OH signal intensity from 308 to 310 nm was integrated). The decomposing rate of naphthalene increased from 32% to 69% when the OH intensity increased from 254.7 to 514.3. The

reason was that higher discharge voltage enhanced the electric field, and thus there were more high-energetic electrons colliding with radical source to generate more OH radicals. Therefore, the decomposing rate of naphthalene increased.

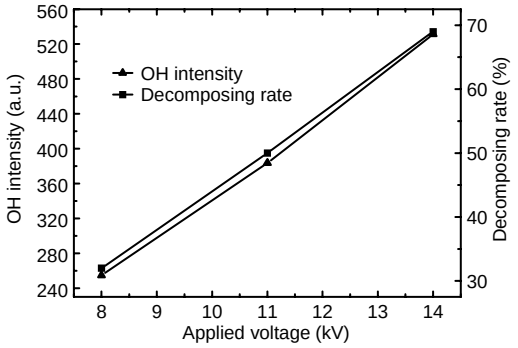

Fig. 5 Influence of applied voltage on OH intensity and decomposing rate

3.1.3 Influence of humidity on naphthalene decomposition

The reaction of $e^*+H_2O\rightarrow OH+H+e$ is an important way to generate OH radicals ($e^*+H_2O\rightarrow OH+H+e$). Therefore, H_2O is useful for OH generation. Conversely, H_2O is also a kind of species for OH quenching. The quenching rate coefficient for OH is expressed as follows (Tamura *et al.*, 1998):

$$k_Q = a_i \sigma_Q T^{0.5}, \tag{3}$$

where a_i is constant for the same gas; σ_Q is the collision cross-section, nm^2; and T is the temperature, K.

For H_2O, a_i=4.92, $\sigma_{Q\text{-}H_2O}$=0.85 nm^2 at T=300 K, so $k_{Q\text{-}H_2O}$=72.4×10^{-11} cm^3/s ($k_{Q\text{-}O_2}$=13.62×10^{-11} cm^3/s; $k_{Q\text{-}N_2}$=2.47×10^{-11} cm^3/s). Therefore, the quenching rate for OH (A) in humid air and dry air was Q_h/Q_d=5.4/4.8. H_2O had a large quenching rate coefficient for OH (A). It was necessary to investigate the influence of humidity on naphthalene decomposition.

In this experiment, the background gas was naphthalene/air with a flow of 5 L/min. The additional gas was humid O_2 with a flow of 0.5 L/min. The initial concentration of naphthalene was 30.5 mg/m^3. As shown in Fig. 6, when the RH increased from 4% to 96% (25 °C, 1.013×10^5 Pa), the decomposing rate increased a little. To investigate the OH radical generation under different humidity, optical emission spectra were shown in Fig. 7. The observed OH wavelength was around 309 nm. The dashed lines represented simulated OH emission spectra with LIFBASE fitted to the respective spectra. OH radicals also increased a little. The reason could be explained as follows: H_2O was helpful to OH generation ($e^*+H_2O\rightarrow OH+H+e$); conversely, it had larger cross section for quenching of the exited OH. Therefore, although the RH increased from 4% to 94%, OH radical generation and decomposing rate did not enhance much.

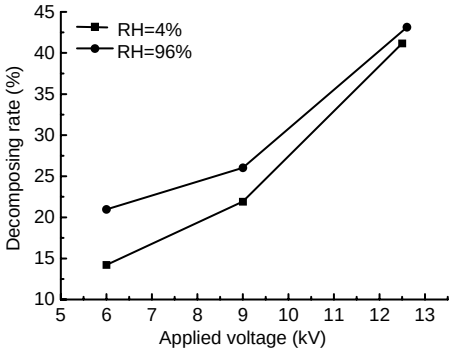

Fig. 6 Naphthalene decomposition under different humid additional gas with the initial naphthalene concentration of 30.5 mg/m^3

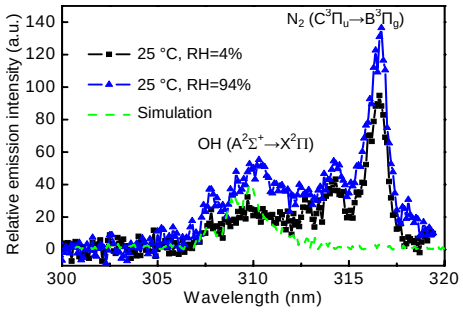

Fig. 7 Emission spectra of OH radicals under different humidities (Gao *et al.*, 2009)

3.2 Analysis of naphthalene decomposing process

3.2.1 Bond energy of naphthalene

The decomposing process of naphthalene in the corona discharge is very complicated. Fig. 8 illustrates the structure of naphthalene (Gao *et al.*, 2009). As shown in Fig. 8, the bond lengths of naphthalene were different (l_I=0.136 nm, l_{II}=0.140 nm, l_{III}=0.139 nm, and l_{IV}=0.142 nm) due to different carbon atoms position. The positions of carbon atoms

numbered 1, 4, 5 and 8 are called α position. The positions of carbon atoms numbered 2, 3, 6 and 7 were called β position. The bond dissociation energy (BDE) calculated by Gaussian 98 is shown in Table 1. The results were similar with the BDE calculated by Reed and Kass (2000) by the B3LYP method (BDE of C_1–H is (469.7±5.4) kJ/mol, and BDE of C_2–H is (468.4±5.9) kJ/mol). Many reactions with radicals occurred in the two bonds. The electron cloud density was higher at α position. Therefore, the reactions always firstly occurred at α position.

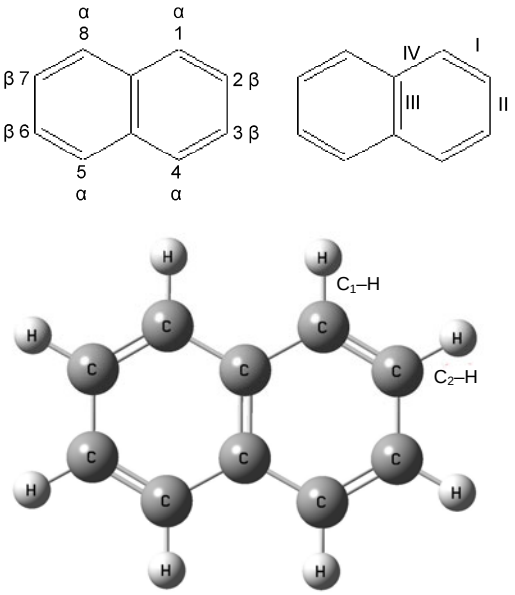

Fig. 8 Structure of naphthalene

l_I=0.136 nm, l_{II}=0.140 nm, l_{III}=0.139 nm, and l_{IV}=0.142 nm

Table 1 Bond dissociation energy (BDE) of naphthalene

Basis set	BDE of C_1–H (kJ/mol)	BDE of C_2–H (kJ/mol)
6–31 G (d, p)	462.33	461.83
6–31+G (d, p)	460.49	460.19
6–31++G (d, p)	456.84	456.59
6–311++G (d, p)	456.34	456.01

3.2.2 Analysis of by-products

The naphthalene decomposition by-products were analyzed by FTIR and GC-MS. The diagnostic peaks of naphthalene were mainly distributed between 3000 and 2800 cm^{-1}. FTIR analysis illustrated in Fig. 9 showed a decline of main naphthalene marker (absorption band around 3100 cm^{-1}) when the applied voltage increased from 0 to 14.5 kV. The standard spectrum of naphthalene was also shown in this figure. Therefore, it was confirmed that a higher voltage was helpful to naphthalene decomposition. FTIR spectra in the CO_2 interference region around 2300 cm^{-1}, the H_2O interference region around 3600 cm^{-1}, and the CO around 2100 cm^{-1} were also observed. According to the previous study (Yu *et al.*, 2010), we believe that there are CO_2, H_2O, and CO generated in the naphthalene decomposing process. In this experiment, the initial naphthalene concentration was 56 mg/m^3. When the applied voltage for GC-MS was 14 kV, the decomposing amount was 19 mg/m^3 and the CO_2 concentration was 43 mg/m^3, so the selectivity for the production of CO_2 was 65.8%. When the applied voltage was 11 kV, the decomposing amount was 13 mg/m^3 and the CO_2 concentration was 29 mg/m^3, so the selectivity for the production of CO_2 was 64.9%. Therefore, the selectivity to the CO_2 value increased with the increase of applied voltage in our experiments.

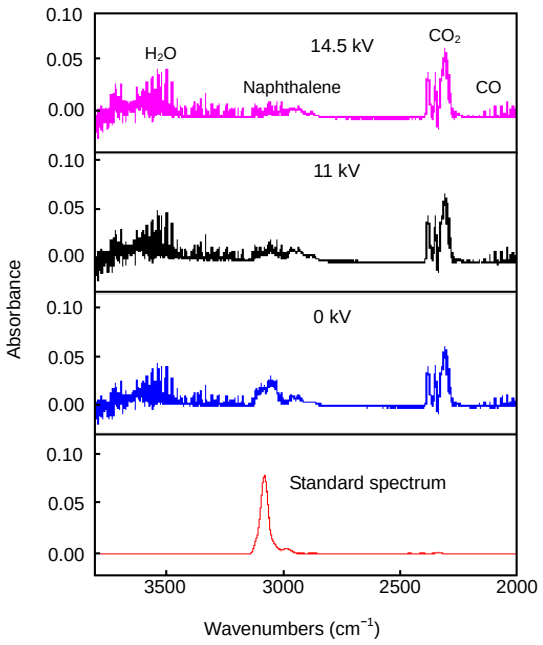

Fig. 9 FTIR spectra of naphthalene decomposition

There may exist other by-products except for CO_2, CO, and H_2O. Therefore, GC-MS was used to distinguish them. GC-MS analyses revealed a series of peaks at different retention times. The by-products generated from 1 to 15 min are listed in Table 2. The

by-products can be classified into three groups: (1) two-ringed compounds; (2) one-ringed compounds; and (3) aliphatic compounds. The possible decomposition pathways in DC CRS discharge will be discussed later based on the experimental results.

Table 2 Main reaction by-products identified by GC-MS

No.	Structure	Name	Retention time (min)
1		Acetaldehyde	1.35
2	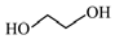	1, 2-ethanediol	1.88
3		4-methyl-3-penten-2-one	2.66
4		Ethanedioic acid, dimethylester	3.06
5		4-hydroxy-4-methyl-2-pentanone	3.26
6		1,2-benzene-dicarboxaldehyde	13.13
7		Phthalide	13.52

3.2.3 Decomposing process of naphthalene in discharge

The decomposing process of naphthalene is a parallel and series-wound process. The possible decomposition pathways of naphthalene are illustrated in Fig. 10. The main products observed by FTIR are CO_2, H_2O, and CO. The reaction intermediate of phthalide can be formed by two pathways shown in Fig. 11 based on Dixon and Longfield (1960). From the calculation in Section 3.2.1, the C–H bond at α position of naphthalene is firstly broken under the effect of radicals such as OH and O. Naphthoquinone is formed via dehydrogenation and oxidation (Vialaton *et al.*, 1999; Onwudili and Williams, 2007; Lair *et al.*, 2008). Subsequently, naphthoquinone can be oxidized into phthalide observed by GC-MS by pathway 3 (Wainwright and Foster, 1979). The phthalide ring can open to form 1,2-benzene-dicarboxaldehyde, and then generate some aliphatic compounds (acetaldehyde, 1,2-ethanediol, etc.). Finally, the aliphatic compounds can be decomposed into inorganic compounds (CO_2, H_2O, CO).

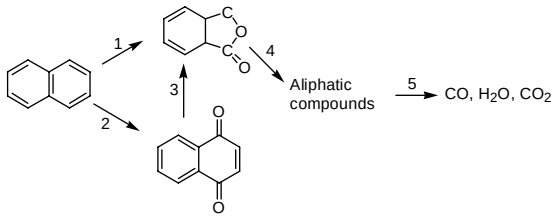

Fig. 10 Naphthalene decomposition process

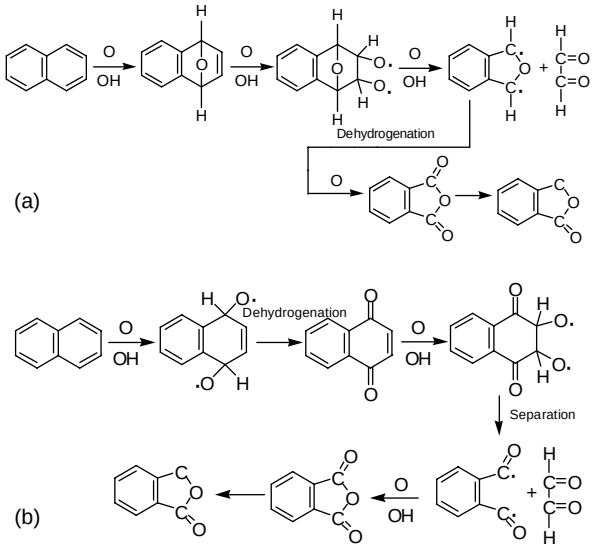

Fig. 11 Main reactions of phthalide formation
(a) Pathway 1; (b) Pathways 2 and 3

4 Conclusions

The naphthalene decomposition in CRS discharge was discussed. High applied voltage and low initial naphthalene density were found to be important to decomposition efficiency. When the initial concentration of naphthalene was 17 mg/m^3, the decomposition rate was 70% under 14 kV. OH ($A^2\Sigma^+ \rightarrow X^2\Pi$) emission spectra have been detected. The H_2O introduction was useful to OH generation. The by-products analysis by FTIR and GC-MS indicated that the main by-products were CO_2 and H_2O. There were also little CO and other small-molecule aliphatic compounds. The naphthalene decomposition was a process of dehydrogenation and oxidation.

References

Aranda, A., Lopez, J.M., Murillo, R., Mastral, A.M., Dejoz, A., Vazquez, I., Solsona, B., Yaylor, S.H., García, T., 2009. Total oxidation of naphthalene with high selectivity using a ceria catalyst prepared by a combustion method

employing ethylene glycol. *Journal of Hazardous Materials*, **171**(1-3):393-399. [doi:10.1016/j.jhazmat.2009.06.013]

Chang, J.S., Urashima, K., Tong, Y.X., Liu, W.P., Wei, H.Y., Yang, F.M., Liu, X.J., 2003. Simultaneous removal of NO_x and SO_2 from coal boiler flue gases by DC corona discharge ammonia radical shower system: pilot plant tests. *Journal of Electrostatics*, **57**(3-4):313-323. [doi:10.1016/S0304-3886(02)00168-7]

de Izarra, C., 2000. UV OH spectrum used as molecular pyrometer. *Journal of Physics D: Applied Physics*, **33**(14):1697-1704.

Dixon, J.K., Longfield, J.E., 1960. Hydrocarbon oxidation. *Catalysis*, **7**:183-280.

Ershov, A., Borysow, J., 1995. Dynamics of OH ($X^2\Pi$, v=0) in high-energy atmospheric pressure electrical pulsed discharge. *Journal of Physics D: Applied Physics*, **28**(1):68-74. [doi:10.1088/0022-3727/28/1/012]

Falkenstein, Z., 1997. Influence of ultraviolet illumination on OH formation in dielectric barrier discharge of $Ar/O_2/H_2O$: the Joshi effect. *Journal of Applied Physics*, **81**(11):7158-7162. [doi:10.1063/1.365313]

Gao, X., Shen, X., Wu, Z.L., Luo, Z.Y., Ni, M.J., Cen, K.F., 2009. The Mechanism of Naphthalene Decomposition in Corona Radical Shower System by DC Discharge. 11th International Conference on Electrostatic Precipitation, Hangzhou, China, p.713-717.

García, T., Solsona, B., Taylor, S.H., 2006. Naphthalene total oxidation over metal oxide catalysts. *Applied Catalysis B: Environmental*, **66**(1-2):92-99. [doi:10.1016/j.apcatb.2006.03.003]

Gong, Z.Q., Alef, K., Wilke, B.M., Li, P.J., 2007. Activated carbon adsorption of PAHs from vegetable oil used in soil remediation. *Journal of Hazardous Materials*, **143**(1-2):372-378. [doi:10.1016/j.jhazmat.2006.09.037]

Hwang, G., Park, S.R., Lee, C.H., Ahn, I.S., Yoon, Y.J., Mhin, B.J., 2009. Influence of naphthalene biodegradation on the adhesion of Pseudomonas putida NCIB 9816-4 to a naphthalene-contaminated soil. *Journal of Hazardous Materials*, **172**(1):491-493. [doi:10.1016/j.jhazmat.2009.07.009]

Lair, A., Ferronato, C., Chovelon, J.M., Herrmann, J.M., 2008. Naphthalene degradation in water by heterogeneous photocatalysis. *Journal of Photochemistry and Photobiology A: Chemistry*, **193**(2-3):193-203. [doi:10.1016/j.jphotochem.2007.06.025]

Mastral, A.M., García, T., Callén, M.S., Navarro, M.V., Galbán, J., 2001. Removal of naphthalene phenanthrene, and pyrene by sorbents from hot gas. *Environmental Science & Technology*, **35**(11):2395-2400. [doi:10.1021/es000152u]

Mista, W., Kacprzyk, R., 2008. Decomposition of toluene using non-thermal plasma reactor at room temperature. *Catalysis Today*, **137**(2-4):345-349. [doi:10.1016/j.cattod.2008.02.009]

Nichipor, H., Dashouk, E., Yacko, S., Chmielewski, A.G., Zimek, Z., Sun, Y., 2002. Chlorinated hydrocarbons and PAH decomposition in dry and humid air by electron beam irradiation. *Radiation Physics and Chemistry*, **65**(4-5):423-427. [doi:10.1016/S0969-806X(02)00352-3]

Nishino, N., Arey, J., Atkinson, R., 2009. Formation and reactions of 2-formylcinnamaldehyde in the OH radical-initiated reaction of naphthalene. *Environmental Science & Technology*, **43**(5):1349-1353. [doi:10.1021/es802477s]

Onwudili, J.A., Williams, P.T., 2007. Reaction mechanisms for the decomposition of phenanthrene and naphthalene under hydrothermal conditions. *The Journal of Supercritical Fluids*, **39**(3):399-408. [doi:10.1016/j.supflu.2006.03.014]

Pellerin, S., Cormier, J.M., Richard, F., Musiol, K., Chapelle, J., 1996. A spectroscopic diagnostic method using UV OH band spectrum. *Journal of Physics D: Applied Physics*, **29**(3):726-739. [doi:10.1088/0022-3727/29/3/034]

Reed, D.R., Kass, S.R., 2000. Experimental determination of α and β C–H bond dissociation energies in naphthalene. *Journal of Mass Spectrometry*, **35**(4):534-539. [doi:10.1002/(SICI)1096-9888(200004)35:4<534::AID-JMS964>3.0.CO;2-T]

Tamura, M., Berg, P.A., Harrington, J.E., Luque, J., Jeffries, J.B., Smith, G.P., Crosley, D.R., 1998. Collisional quenching of CH (A), OH (A) and NO (A) in low pressure hydrocarbon flames. *Combustion and Flame*, **114**(3-4):502-514. [doi:10.1016/S0010-2180(97)00324-6]

Urashima, K., Chang, J.S., 2000. Removal of volatile organic compounds from air streams and industrial flue gases by non-thermal plasma technology. *IEEE Transactions on Dielectrics and Electrical Insulation*, **7**(5):602-614. [doi:10.1109/94.879356]

Vialaton, D., Richard, C., Baglio, D., 1999. Mechanism of the photochemical transformation of naphthalene in water. *Journal of Photochemistry and Photobiology A: Chemistry*, **123**(1-3):15-19. [doi:10.1016/S1010-6030(99)00044-1]

Wainwright, M.S., Foster, N.R., 1979. Catalysis, kinetics, and reactor design in phthalic anhydride synthesis. *Catalysis Reviews*, **19**(2):211-292. [doi:10.1080/03602457908068056]

Wu, Z.L., Gao, X., Luo, Z.Y., Wei, E.Z., Zhang, Y.S., Zhang, J.Z., Ni, M.J., Cen, K.F., 2005. NO_x treatment by DC corona radical shower with different geometric nozzle electrodes. *Energy & Fuels*, **19**(6):2279-2286. [doi:10.1021/ef0400823]

Yu, L., Li, X.D., Tu, X., Wang, Y., Lu, S.Y., Yan, J.H., 2010. Decomposition of naphthalene by DC gliding arc gas discharge. *The Journal of Physical Chemistry A*, **114**(1):360-368. [doi:10.1021/jp905082s]